# Neuronal adaptor FE65 stimulates Rac1-mediated neurite outgrowth by recruiting and activating ELMO1

Received for publication, October 17, 2017, and in revised form, March 12, 2018 Published, Papers in Press, April 3, 2018, DOI 10.1074/jbc.RA117.000505

**Wen Li, Ka Ming Vincent Tam, Wai Wa Ray Chan, Alex Chun Koon, Jacky Chi Ki Ngo, Ho Yin Edwin Chan, and Kwok-Fai Lau**[1]

*From the School of Life Sciences, Faculty of Science, Chinese University of Hong Kong, Shatin New Territories, Hong Kong*

Edited by Peter Cresswell

**Neurite outgrowth is a crucial process in developing neurons for neural network formation. Understanding the regulatory mechanisms of neurite outgrowth is essential for developing strategies to stimulate neurite regeneration after nerve injury and in neurodegenerative disorders. FE65 is a brain-enriched adaptor that stimulates Rac1-mediated neurite elongation. However, the precise mechanism by which FE65 promotes the process remains elusive. Here, we show that ELMO1, a subunit of ELMO1-DOCK180 bipartite Rac1 guanine nucleotide exchange factor (GEF), interacts with the FE65 N-terminal region. Overexpression of FE65 and/or ELMO1 enhances, whereas knockdown of FE65 or ELMO1 inhibits, neurite outgrowth and Rac1 activation. The effect of FE65 alone or together with ELMO1 is attenuated by an FE65 double mutation that disrupts FE65-ELMO1 interaction. Notably, FE65 is found to activate ELMO1 by diminishing ELMO1 intramolecular autoinhibitory interaction and to promote the targeting of ELMO1 to the plasma membrane, where Rac1 is activated. We also show that FE65, ELMO1, and DOCK180 form a tripartite complex. Knockdown of DOCK180 reduces the stimulatory effect of FE65-ELMO1 on Rac1 activation and neurite outgrowth. Thus, we identify a novel mechanism by which FE65 stimulates Rac1-mediated neurite outgrowth by recruiting and activating ELMO1.**

FE65 is a brain-enriched adaptor protein with several protein interaction domains, including a WW domain and two C-terminal PTB[2] domains (see Fig. 1*A*). It is generally believed that FE65 acts as a "scaffold" protein to recruit various interactors to form a functional complex. Indeed, a number of FE65-interacting proteins (FIPs) are identified for its conserved domains. These findings have provided insights into the biological functions of FE65. For instance, FE65, via its PTB2 domain, is shown to interact with Alzheimer's disease amyloid precursor protein (APP) and to alter APP processing. Moreover, the FE65 PTB1 domain is found to interact with the small GTPase ARF6 (reviewed in Refs. 1 and 2).

Additionally, FE65 is implicated in neurodevelopment. FE65 knockout mice have been shown to have significant impairment in hidden-platform acquisition ability and reversal learning (3). Increased neonatal mortality and abnormal circling behavior are reported for FE65/FE65L1 double knockout mice. In fact, aberrant laminin organization of meningeal fibroblasts and axonal projection and pathfinding impairments in several brain regions have been observed in the mice (4). Moreover, neuromuscular junction abnormalities and long-term potentiation impairments are observed in the mice (5). We have also shown that FE65 stimulates neurite outgrowth, an essential process for neural network formation, by activating ARF6-Rac1 signaling (6). Because FE65 does not possess any guanine nucleotide exchange factor (GEF) catalytic activity, the underlying mechanisms by which FE65 stimulates the signaling pathway remain elusive. Nevertheless, the above findings underscore FE65 plays significant developmental roles in the nervous system.

Despite the fact that a number of interactors for the conserved domains are identified, FE65 N-terminal region (NTR) binding partners have not been properly determined yet. As an adaptor, it is possible that FE65 NTR is also involved in protein recruitment. To this end, we performed a yeast two-hybrid screen using FE65 NTR as "bait" and identified engulfment and cell motility protein 1 (ELMO1) as a novel FE65 interactor.

ELMO1 is a ubiquitously expressed protein containing an N-terminal Ras-binding domain, an ELMO inhibitory domain (EID), an ELMO domain, a pleckstrin homology domain, an ELMO autoregulatory domain (EAD), and a C-terminal P*XX*P motif (Fig. 1*A*) (reviewed in Ref. 7). ELMO1 is reported to be involved in various processes, including phagocytosis, cell migration, cancer metastasis, dendritic spine morphogenesis, and lymphocyte migration (reviewed in Refs. 8 and 9–11). Many of these processes require dynamic remodeling of the actin cytoskeleton. The effects of ELMO1 are attributable, at least in part, to Rac1, a member of the Rho GTPases that regulate actin dynamics. Rac1 is activated by the GEFs, which promote the exchange of GDP to GTP in Rac1. By contrast,

This work was supported by funds from the Research Grants Council Hong Kong, Health and Medical Research Fund (Hong Kong), CUHK direct grant scheme, the United College endowment fund, and the TUYF Charitable Trust. The authors declare that they have no conflicts of interest with the contents of this article.

[1] To whom correspondence should be addressed. Tel.: 852-39431106; Fax: 852-26037246; E-mail: kflau@cuhk.edu.hk.

[2] The abbreviations used are: PTB, phosphotyrosine-binding; APP, amyloid precursor protein; ARF6, ADP-ribosylation factor 6; CHO, Chinese hamster ovary; DOCK180, dedicator of cytokinesis 180; ELMO1, engulfment and cell motility protein 1; GEF, guanine nucleotide exchange factor; GST, glutathione *S*-transferase; HEK, human embryonic kidney; PM, plasma membrane; NTR, N-terminal region; EID, ELMO inhibitory domain; ICA, intensity correlation analysis; ICQ, intensity correlation quotient; PLA, proximity ligation assay; Y2H, yeast two-hybrid; E18, embryonic day 18; EGFP, enhanced green fluorescent protein; GAPDH, glyceraldehyde-3-phosphate dehydrogenase; DAPI, 4′,6-diamidino-2-phenylindole; IP, immunoprecipitation.

GTPase-activating proteins inactivate Rac1 by promoting GTP hydrolysis (reviewed in Ref. 12). In cells, ELMO1 complexes with DOCK180 to form a bipartite GEF in cells awaiting the yet to be identified activation signal(s) to mediate Rac1-dependent cytoskeleton remodeling (7, 13, 14). Here, we show that FE65 interacts with ELMO1 and in turn diminishes ELMO1 intramolecular autoinhibitory interaction. Moreover, FE65-ELMO1 interaction plays a role in stimulating Rac1-mediated neurite outgrowth.

## Results

### *FE65 interacts directly with ELMO1*

From a yeast two-hybrid screen of a mouse brain cDNA library using FE65(1–217) fragment as "bait," a cDNA clone encoding ELMO1(626–727), which contains part of the pleckstrin homology domain, EAD, and the P*XX*P motif, was isolated. Their interaction in yeast was confirmed using a $\beta$-gal colony-lift filter assay (Fig. 1*B*).

To further analyze the FE65-ELMO1 interaction, bacterially expressed GST and GST-ELMO1(626–727) fusion proteins were used as baits to pull down FE65 from transfected cells. In this assay, ELMO1(626–727), but not GST, pulled down FE65 (Fig. 1*C*). We next tested the FE65-ELMO1 interaction by using immunoprecipitation assays from transfected cells. FE65 was transfected either alone or co-transfected with Myc-tagged ELMO1. ELMO1 was then immunoprecipitated via the Myc tag. FE65 was detected in immunoprecipitates from the FE65 + ELMO1 but not FE65 singly transfected control cells (Fig. 1*D*). To demonstrate that endogenous FE65-ELMO1 interaction, we immunoprecipitated ELMO1 from rat brains and probed the immunoprecipitate for FE65. As shown in Fig. 1*E*, both ELMO1 and FE65 were present in the immunoprecipitates.

The above biochemical assays indicate that FE65 interacts with ELMO1. However, they could not exclude the possibility that FE65-ELMO1 interaction is mediated by an intermediate molecule. To examine whether this interaction is direct, we incubated *Escherichia coli* purified His-FE65(1–217) with *E. coli* purified GST or GST-ELMO1(626–727) baits. As shown in Fig. 1*F*, His-FE65(1–217) could be pulled down by GST-ELMO1(626–727) but not GST. Taken together, these results demonstrate that FE65 interacts directly with ELMO1.

Next, we determined the regions in FE65 and ELMO1 that mediate their interaction. In addition to FE65(1–217), we further prepared three FE65 NTR yeast "bait" constructs. Yeast cells were co-transformed with ELMO1(626–727) prey construct and different FE65 NTR baits and then grown on double and quadruple dropout SD agar plates. We found that the transformants could not grow on a quadruple dropout plate when FE65 amino acids 1–60 were deleted (Fig. 1*G*, *top*). This suggests that the first 60 residues of FE65 are essential for FE65-ELMO1 interaction. We then determined the residue(s) in FE65 that is critical for mediating FE65-ELMO1 interaction by generating a number of FE65 mutants and tested their abilities to interact with ELMO1 in co-immunoprecipitation assays. We found that FE65 Lys-48 and Arg-51 (FE65m) are crucial for FE65-ELMO1 interaction, as the interaction was markedly reduced by an FE65 K48A/R51A double mutation (Fig. 1*H*).

On the other hand, ELMO1(626–680) could not interact with FE65(1–217) in yeast two-hybrid assay (Fig. 1*G*, *bottom*). This suggests that amino acids 681–727 of ELMO1, which contain EAD and P*XX*P, are required for the interaction. ELMO1 Met-692 and Glu-693 are two critical residues in EAD for mediating protein interaction, at least with ELMO1 EID (15). Therefore, we tested whether the two residues are essential for FE65-ELMO1 interaction. As shown in Fig. 1*G*, an ELMO1 M692A/E693A (ELMO1m) double mutation abolished the interaction between ELMO1(626–727) and FE65(1–217) in the yeast two-hybrid system. We confirmed the importance of the two residues by a co-immunoprecipitation assay in which FE65-ELMO1 interaction was markedly reduced by an ELMO1m double mutation (Fig. 1*I*). Together, our result suggests that FE65(1–60) and ELMO1 EAD are required for FE65-ELMO1 interaction.

### *FE65 and ELMO1 promote neurite outgrowth and Rac1 activation*

Previously, we have found that FE65 stimulates Rac1-dependent neurite outgrowth (6). Because ELMO1 also enhances Rac1 activation and is widely expressed in different cell types, including neurons (Fig. 2*A*), we anticipated that FE65-ELMO1 interaction promotes neurite extension. To test this, 2 days *in vitro* rat primary cortical neurons were transfected with FE65, ELMO1, and FE65 + ELMO1 together with enhanced GFP-expressing plasmid (pEGFP-C1), which serves as a morphology marker for the transfected neurons. The expressions of FE65 and/or ELMO1 were confirmed by both Western blotting and immunofluorescence analyses (Fig. 2*B*, *top right* and *bottom*). The lengths of the longest neurite from the growth cone tip to the periphery of the cell body of the transfected neurons were measured 24 h post-transfection. This is a widely employed neurite measurement approach (*e.g.* see Refs. 6, 16, and 17). Similar to our previous report (6), overexpression of FE65, but not FE65m, stimulated neurite extension (Fig. 2*B*, *top left*). Notably, overexpression of ELMO1 also promoted neurite outgrowth (Fig. 2*B*). As we have shown that ELMO1 interacts with FE65 (Fig. 1) and FE65 is expressed in neurons (Fig. 2*A*), the effect of overexpression of ELMO1 on neurite outgrowth might be due to the transfected ELMO1 that interacted with endogenous FE65 in the neurons. In fact, a more pronounced stimulatory effect was observed in FE65 + ELMO1 co-transfected neurons, and such an effect was not observed in FE65m + ELMO1 (Fig. 2*B*). As FE65m could not interact with ELMO1 properly, our findings suggest that FE65-ELMO1 interaction could promote neurite outgrowth.

Rac1 is a key regulator of actin cytoskeleton dynamics that controls a number of developmental events in neurons, including neurite outgrowth (for a review, see Ref. 18). We therefore investigated whether FE65-ELMO1 interaction influences Rac1 activity. As shown in Fig. 3*A*, overexpression of FE65 or ELMO1 could activate Rac1. However, FE65m could not stimulate Rac1. Of note, Rac1 was strongly activated in FE65 + ELMO1, but not FE65m + ELMO1, co-transfected cells (Fig. 3*A*). Because FE65m has reduced binding ability

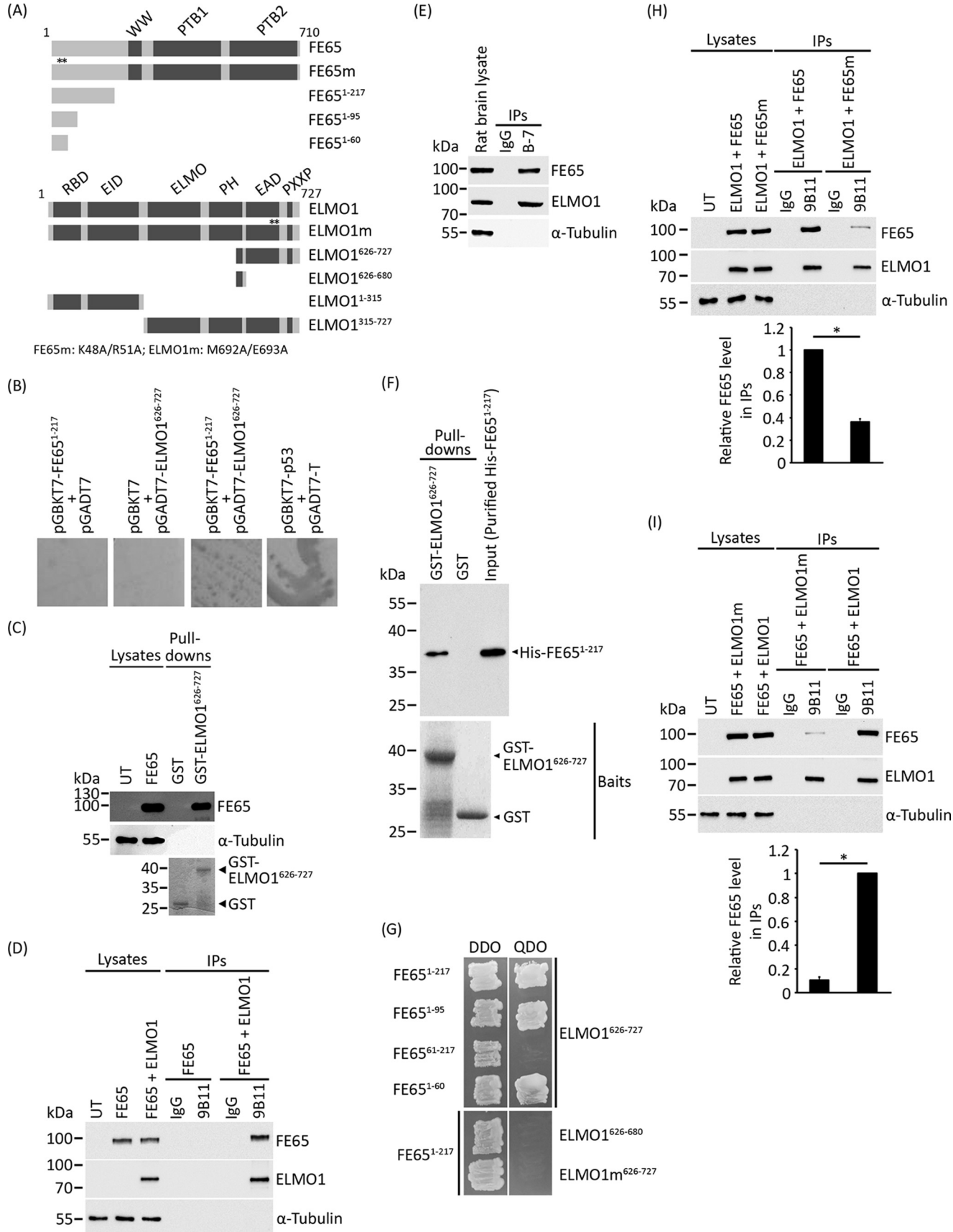
(A)
WW
PTB1
PTB2
FE65
FE65m
FE65^1-217
FE65^1-95
FE65^1-60
RBD
EID
ELMO
PH
EAD
PXXP
ELMO1
ELMO1m
ELMO1^626-727
ELMO1^626-680
ELMO1^1-315
ELMO1^315-727
FE65m: K48A/R51A; ELMO1m: M692A/E693A
(B)
pGBKT7-FE65^1-217 + pGADT7
pGBKT7 + pGADT7-ELMO1^626-727
pGBKT7-FE65^1-217 + pGADT7-ELMO1^626-727
pGBKT7-p53 + pGADT7-T
(C)
Lysates
Pull-downs
UT
FE65
GST
GST-ELMO1^626-727
kDa
FE65
α-Tubulin
GST-ELMO1^626-727
GST
(D)
Lysates
IPs
UT
FE65
FE65 + ELMO1
IgG
9B11
kDa
FE65
ELMO1
α-Tubulin
(E)
Rat brain lysate
IPs
IgG
B-7
kDa
FE65
ELMO1
α-Tubulin
(F)
Pull-downs
GST-ELMO1^626-727
GST
Input (Purified His-FE65^1-217)
kDa
His-FE65^1-217
GST-ELMO1^626-727
GST
Baits
(G)
DDO
QDO
FE65^1-217
FE65^1-95
FE65^61-217
FE65^1-60
ELMO1^626-727
FE65^1-217
ELMO1^626-680
ELMO1m^626-727
(H)
Lysates
IPs
UT
ELMO1 + FE65
ELMO1 + FE65m
IgG
9B11
kDa
FE65
ELMO1
α-Tubulin
Relative FE65 level in IPs
(I)
Lysates
IPs
UT
FE65 + ELMO1m
FE65 + ELMO1
IgG
9B11
kDa
FE65
ELMO1
α-Tubulin
Relative FE65 level in IPs

toward ELMO1, our findings suggest that FE65-ELMO1 plays a role in promoting Rac1 activation.

To further dissect the roles of FE65 and ELMO1 in neurite outgrowth, an siRNA knockdown approach was employed. Akin to our previous finding (6), knockdown of FE65 reduced the basal neurite extension significantly (Fig. 2*C*). A similar effect was observed in ELMO1 knockdown neurons (Fig. 2*C*). These observations further suggest that both FE65 and ELMO1 are essential for neurite outgrowth. Intriguingly, the stimulatory effect of overexpression of ELMO1 on neurite outgrowth and Rac1 were markedly reduced in FE65 knockdown cells (Figs. 2*D* and 3*B*). This suggests that FE65 is required, at least in part, for the effects of ELMO1 on neurite outgrowth and Rac1 activation. On the other hand, overexpression of FE65 could not stimulate neurite growth in ELMO1 knockdown neurons (Fig. 2*E*), and its effect on Rac1 activation was also decreased markedly in ELMO1 knockdown cells (Fig. 3*C*). Collectively, our findings suggest that FE65 plays a role, at least in part, in stimulating Rac1-mediated neurite outgrowth by interacting with ELMO1.

### *DOCK180 is required for FE65- and ELMO1-mediated Rac1 activation and neurite outgrowth*

As stated before, ELMO1 is a subunit of the ELMO1-DOCK180 bipartite Rac1 GEF complex (13). We therefore determined whether FE65 alters the GEF complex formation. To do this, FLAG-DOCK180 was precipitated by anti-FLAG M2 antibody from DOCK180 + ELMO1- and DOCK180 + ELMO1 + FE65-transfected cell lysates. As shown in Fig. 4*A*, the amounts of ELMO1 in both immunoprecipitates were similar. Notably, FE65 was also detected in the immunoprecipitate from ELMO1 + DOCK180 + FE65-transfected cell lysate (Fig. 4*A*). Moreover, we were able to determine a tripartite complex of DOCK180, ELMO1, and FE65 at the endogenous level by immunoprecipitating DOCK180 from rat brain lysate (Fig. 4*B*). Taken together, both FE65 and DOCK180 can bind simultaneously to ELMO1 to form a tripartite complex.

Because DOCK180 is the catalytic subunit of ELMO1-DOCK180 bipartite Rac1 GEF complex (13), we tested whether DOCK180 was essential for FE65-mediated Rac1 activation. Similar to our previous observation, overexpression of FE65 activated Rac1 (Fig. 4*C*). However, the effect of FE65 on Rac1 activation was reduced significantly in DOCK180 knockdown cells (Fig. 4*C*). Similarly, knockdown of DOCK180 decreased the effect of ELMO1 on Rac1 activation (Fig. 4*C*). The combined effect of FE65 and ELMO1 on Rac1 was also markedly lowered in DOCK180 knockdown cells (Fig. 4*C*).

We also determined the effect of DOCK180 knockdown on FE65-ELMO1-mediated neurite extension. As shown in Fig. 4*D*, knockdown of DOCK180 reduced the stimulating effects of FE65, ELMO1, and FE65 + ELMO1 on neurite outgrowth. Together, our results suggest that DOCK180 is required, at least in part, for FE65-ELMO1–mediated Rac1 activation and neurite outgrowth.

### *FE65 and ELMO1 co-localize on the plasma membrane and neuronal growth cones*

To interact in cells, FE65 and ELMO1 must be located within the same subcellular compartment. Because Rac1 is mainly activated on the plasma membrane (19), and both FE65 and ELMO1 stimulate Rac1, we determined whether FE65 and ELMO1 are expressed on the plasma membrane. Plasma membrane was prepared from both FE65 + ELMO1 co-transfected cells and primary cortical neurons by using a Qproteome plasma membrane protein kit (Qiagen). Approximately 30% of plasma membrane elution and 1% total lysate (as size control) were subjected to immunoblotting for FE65, ELMO1, and various subcellular compartment markers. We found that both FE65 and ELMO1 were detected in the plasma membrane elutions from FE65 + ELMO1 co-transfected cells (Fig. 5*A*) and primary cortical neurons (Fig. 5*B*).

The above biochemical plasma membrane isolation revealed the presence of both FE65 and ELMO1 in the plasma membrane elutions, and we further analyzed whether the two proteins are co-localized in cells by confocal microscopy. In fact, FE65 and ELMO1 were found co-localized in the perinuclear region of FE65 + ELMO1 co-transfected cells. Noteworthy, a proportion of ELMO1 and FE65 was observed co-localized on

**Figure 1. FE65 interacts with ELMO1.** *A*, schematic diagrams to show the various subdomains and mutants of FE65 and ELMO1 used in this study. *Asterisks*, positions of mutations in FE65 and ELMO1. *B*, FE65(1–217) interacts with ELMO1(626–727) in a yeast two-hybrid system. pGBKT7-FE65(1–217) + pGADT7, pGBKT7 + pGADT7-ELMO1(626–727), pGBKT7-FE65(1–217) + pGADT7-ELMO1(626–727), and pGBKT7-p53 + pGADT7-T were transformed into the yeast strain Y2H Gold and grew on quadruple (−Ade/−His/−Leu/−Trp; QDO) dropout SD agar plates. Colony lift assays were performed for the transformants. Blue signals were observed in yeast transformed with pGBKT7-FE65(1–217) + pGADT7-ELMO1(626–727) and pGBKT7-p53 + pGADT7-T (positive control). *C*, ELMO1 binds to FE65 in GST pulldown assays. *E. coli* expressed GST and GST-ELMO1(626–727) were used as baits in pulldown assays from FE65-transfected cells. FE65 in the cell lysates and pulldowns was detected by using goat anti-FE65 E20 antibody (1:5000). Coomassie blue gel showed the GST and GST-ELMO1 baits. *D*, FE65 and ELMO1 interact in immunoprecipitation assays from transfected cells. Immunoprecipitations were performed from CHO cells transfected with FE65- or FE65 + Myc-tagged ELMO1. ELMO1 was immunoprecipitated using anti-Myc antibody 9B11. Immunoprecipitated FE65 and ELMO1 were detected by a goat anti-FE65 (1:5000) and a rabbit anti-Myc (1:5000), respectively. *IgG* and *9B11* refer to the presence of mouse control IgG and Myc antibody 9B11 in the immunoprecipitations, respectively. *E*, FE65 interacts endogenously with ELMO1. ELMO1 was immunoprecipitated from rat brain lysate using mouse anti-ELMO1 B-7. Immunoprecipitated ELMO1 and FE65 were detected using rabbit anti-ELMO1 antibody PA5–28406 (1:500) and goat anti-FE65 E20 antibody (1:1000), respectively. *IgG* and *B-7* refer to the presence of mouse control IgG and anti-ELMO1 in the immunoprecipitations, respectively. *F*, FE65 interacts directly with ELMO1. *E. coli* expressed GST and GST-ELMO1(626–727) were used to pull down purified His-tagged FE65(1–217). *Bottom*, recombinant bait proteins in the pulldowns; *top*, pulldowns and the purified His-tagged FE65(1–217). *G*, FE65(1–60) and ELMO1(680–727) are essential for FE65-ELMO1 interaction. FE65(1–217), FE65(1–95), FE65(61–217), and FE65(1–60) were cloned into pGBKT7. ELMO1(626–727), ELMO1(626–680), and ELMO1(626–727)$^{M692A/E693A}$ (ELMO1m(627–727)) were cloned into pGADT7. FE65 and ELMO1 constructs were co-transformed into yeast Y2H Gold. The transformants were grown on double (−Leu/−Trp; DDO) and quadruple (−Ade/−His/−Leu/−Trp; QDO) dropout SD agar plates. FE65 Lys-48 and Arg-51 (*H*) and ELMO1 Met-692 and Glu-693 (*I*) are crucial residues for the interaction. Myc-tagged ELMO1 was immunoprecipitated from the transfected lysates using anti-Myc 9B11. ELMO1 and FE65 in the immunoprecipitates were detected using rabbit anti-ELMO1 antibody (1:5000) and goat anti-FE65 antibody E20 (1:5000), respectively. *IgG* and *B-7* refer to the presence of mouse control IgG and anti-ELMO1 in the immunoprecipitations, respectively. Lysates and pulldown/IP samples in *C*, *D*, *E*, *F*, *H*, and *I* were probed with anti-α-tubulin DM1A antibody (1:5000) to illustrate lysate loading and pulldowns/IP specificity, respectively. FE65 and ELMO1 levels were measured by a C-DiGit blot scanner (LI-COR) and analyzed by LI-COR® Image Studio™ software. Data for graphs in *H* and *I* were obtained from independent experiments. $n = 3$. *, $p < 0.001$. Results are means ± S.D.

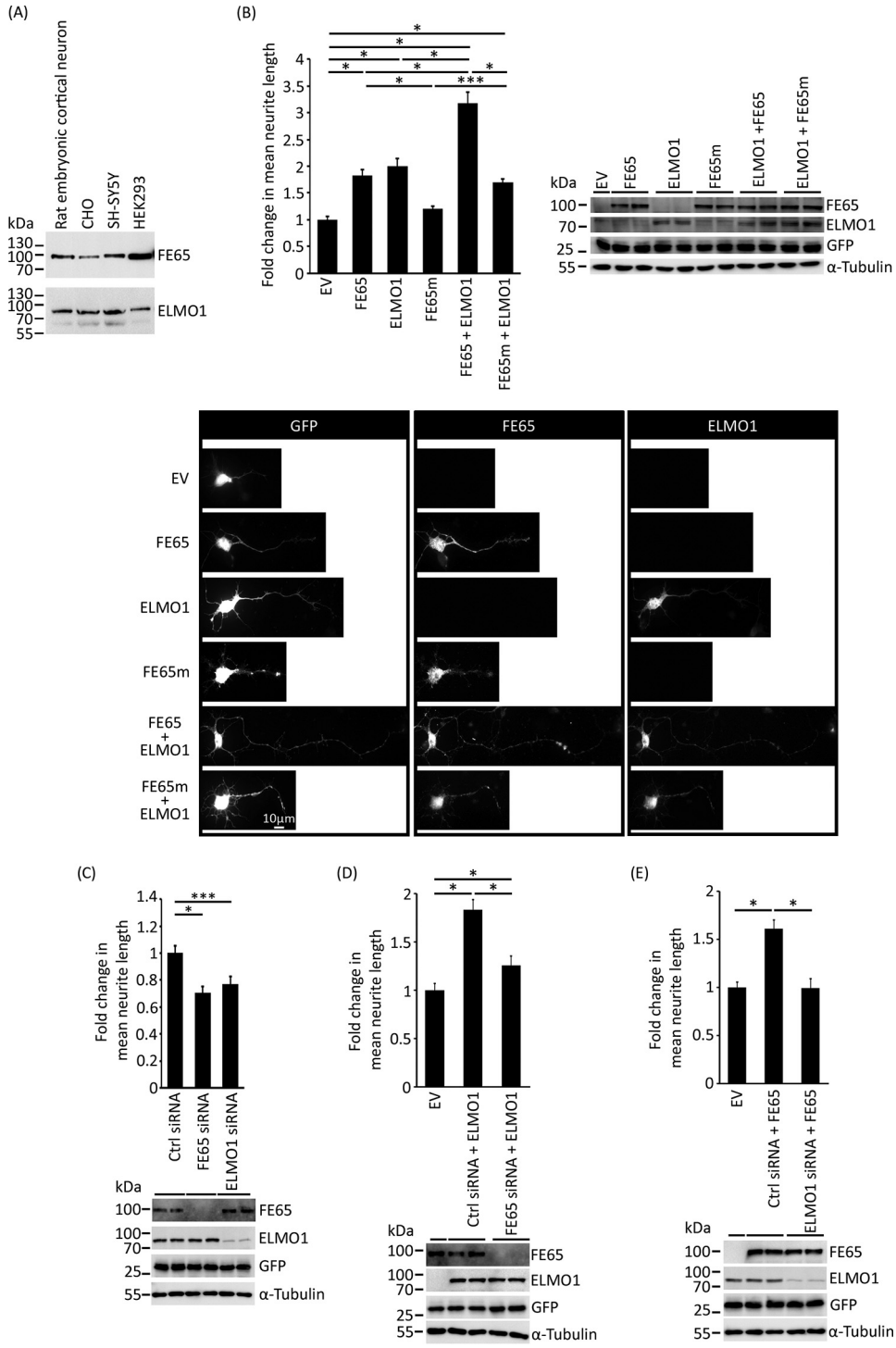


**Figure 2. FE65-ELMO1 interaction stimulates neurite outgrowth.** *A*, Western blots to show the expression of FE65 and ELMO1 in different cell types. Approximately 10 $\mu$g of lysate from E18 rat embryonic cortical neurons, CHO, SH-SY5Y, and HEK293 cells were loaded. FE65 and ELMO1 were detected by anti-FE65 E20 (1:1000) and anti-ELMO1 B-7 (1:500), respectively. *B–E*, rat primary cortical neurons were transfected with EGFP as a cell morphology marker and different combinations of FE65 and ELMO1 constructs and either control, FE65, or ELMO1 siRNAs, as indicated. All transfections received the same amounts of DNA. The length of the longest neurite was then determined 24 h later. Bar charts show -fold changes in mean neurite length for the longest neurite. Representative images of the different transfected cells are shown for *B*. FE65-Myc and Myc-ELMO1 were stained with a rabbit anti-FE65 (1:500) and mouse anti-ELMO1 B-7 (1:1000), respectively. *Scale bar*, 10 $\mu$m. The expressions of EGFP and FE65-Myc/Myc-ELMO1 were also determined by Western blot analysis using anti-GFP JL-8 (1:5000) and anti-Myc 9B11 (1:2500), respectively. $\alpha$-Tubulin in the lysates was determined by anti-$\alpha$-tubulin DM1A antibody (1:5000). Both FE65 and ELMO1 enhance neurite outgrowth. More potent effects are observed in FE65 + ELMO1, but not in FE65m + ELMO1, co-transfected cells (*B*). Knockdown of either FE65 or ELMO1 reduces the basal neurite extension in the cortical neurons (*C*). Knockdown of FE65 reduces the effect of ELMO1 on neurite outgrowth (*D*). Knockdown of ELMO1 suppresses the effect of FE65 on neurite outgrowth (*E*). In *B–E*, data were obtained from at least 40 cells per transfection, and the experiments were repeated three times. *, $p < 0.001$; ***, $p < 0.05$. *Error bars*, S.E.

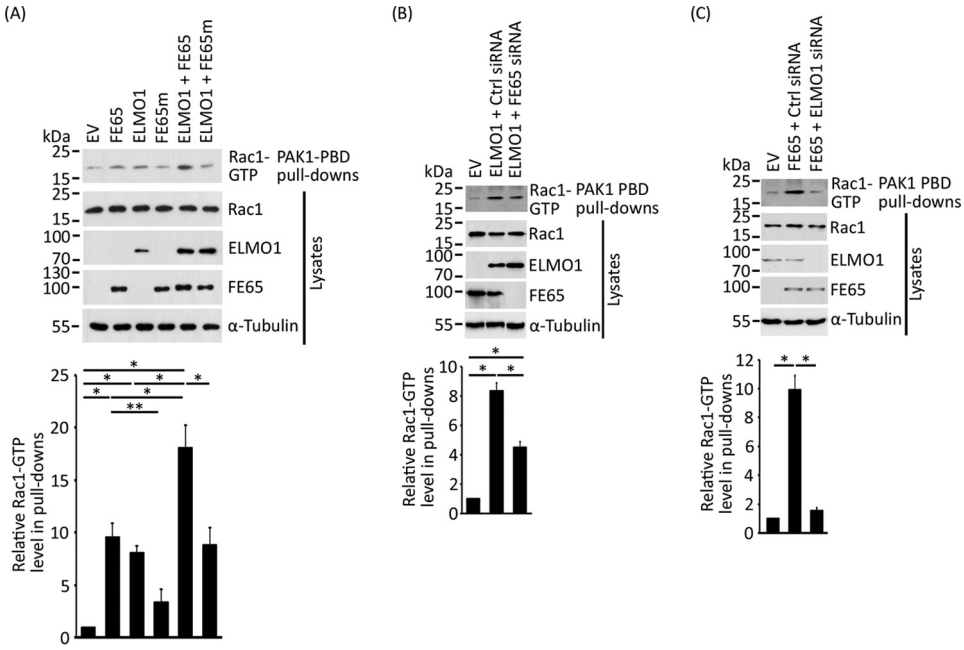


**Figure 3. FE65-ELMO1 interaction activates Rac1.** *A–C*, CHO cells were transfected with the constructs EV control plasmid, FE65, FE65m, and ELMO1 and either control, FE65, or ELMO1 siRNAs as indicated. Active Rac1 was pulled down from the transfected cell lysates using GST-PAK1 PBD bait (supplied in the Rac1 activation assay kit (Thermo Fisher Scientific)), which binds Rac1-GTP. Rac1-GTP bound to the bait was analyzed on immunoblots using anti-Rac1 23A8 (1:5000), FE65 E20 (1:5000), Rac1 23A8 (1:5000), ELMO1 B-7 (1:5000), and α-tubulin DM1A (1:5000), and expression levels in the cell lysates are also shown. Both FE65 and ELMO1 enhance Rac1 activation. More potent effects are observed in FE65 + ELMO1, but not FE65m + ELMO1, co-transfected cells (*A*). Knockdown of FE65 decreases the effect of ELMO1 on Rac1 activation (*B*). Knockdown of ELMO1 reduces the effect of FE65 on Rac1 activation (*C*). In *A–C*, the relative Rac1-GTP level was expressed as a densitometric ratio of Rac1-GTP/total Rac1. Data for graphs were obtained from three independent experiments. *, $p < 0.001$; **, $p < 0.01$. Results are means ± S.D. (*error bars*).

the plasma membrane (Fig. 5*C*). We also determined whether there was significant overlap in the distribution of the two proteins on plasma membrane by intensity correlation analysis (ICA) (6, 20, 21). The reporting intensity correlation quotient (ICQ) is statistically testable. For random staining, ICQ = 0; for dependent staining (co-localization), $0 < \text{ICQ} < +0.5$; for segregated staining, $-0.5 < \text{ICQ} < 0$. ICAs revealed a significant co-localization of FE65 and ELMO1 on the plasma membrane (mean ± S.E.; ICQ = 0.15 ± 0.01, $p < 0.001$; $n = 40$).

In rat cortical neurons, both distinct and overlapping staining were detected (Fig. 5*D*), in particular at the cell bodies. In fact, ICA at the cell bodies indicated a moderate covariance (ICQ = 0.054 ± 0.02; $p < 0.001$; $n = 40$). Because Rac1 is a regulator of actin cytoskeletal dynamics of growth cones at the tip of growing neurites (18, 22, 23), and FE65 potentiates the effect of ELMO1 on Rac1 activation, we also enquired whether FE65 and ELMO1 co-localize in the growth cones of neurons. Akin to previous reports (6, 24), FE65 was observed at the growth cones. Importantly, ELMO1 immunostain signal overlapped significantly with FE65 in the growth cones (ICQ = 0.26 ± 0.01; $p < 0.001$; $n = 40$) (Fig. 5*D*).

### *FE65 releases ELMO1 autoinhibitory conformation and promotes plasma membrane targeting of ELMO1*

ELMO1 is shown to adopt a closed autoinhibitory conformation via intramolecular interaction between its N-terminal EID and C-terminal EAD that plays a role in regulating Rac1 signaling (15). It is proposed that the relief of ELMO1 autoinhibition is a prerequisite for targeting ELMO1-DOCK180 complex to the plasma membrane. Moreover, although yet to be identified, ELMO1 C-terminal interactors are suggested to play a role in Rac1 signaling by releasing ELMO1 autoinhibition constraints (7, 13). Because our data reveal that FE65 interacts with the C terminus of ELMO1, we tested whether FE65 influences ELMO1 EID-EAD interaction. Mammalian expression constructs of Myc-ELMO1(1–315) and GST-ELMO1(315–727) were transfected to the cells with empty vector (EV), FE65, or FE65m. GST-ELMO1(315–727) was captured from the cell lysates by GSH-Sepharose 4B resin. Similar to the previous report, GST-ELMO1(1–315) bound to ELMO1(315–727) in the pulldown assay. Intriguingly, GST-ELMO1(315–727) could not pull down ELMO1(1–315) when co-transfected with FE65 but not FE65m mutant (Fig. 6*A*). Because FE65m interacts less with ELMO1 (Figs. 1*H* and 6*A* (*bottom*)), our data may suggest that FE65 interferes with ELMO1 EID-EAD interaction by competing with ELMO1 N-terminal EID for binding to the C-terminal EAD.

To confirm that FE65 disrupts ELMO1 autoinhibition conformation, proximity ligation assays (PLAs) were performed for ELMO1(1–315) and ELMO1(315–727) in cells. Mammalian expression constructs for Myc-ELMO1(1–315) and FLAG-ELMO1(315–727) were transfected into the cells with EV, FE65, or FE65m. As shown in Fig. 6*B*, fluorescence PLA signals were observed in cells transfected with ELMO1(1–315) and ELMO1(315–727), which suggests that the two ELMO1 fragments interacted in cells. Upon co-transfection with FE65, but not FE65m, the number of PLA signals was significantly reduced in cells. No detectable signal was found in control PLAs

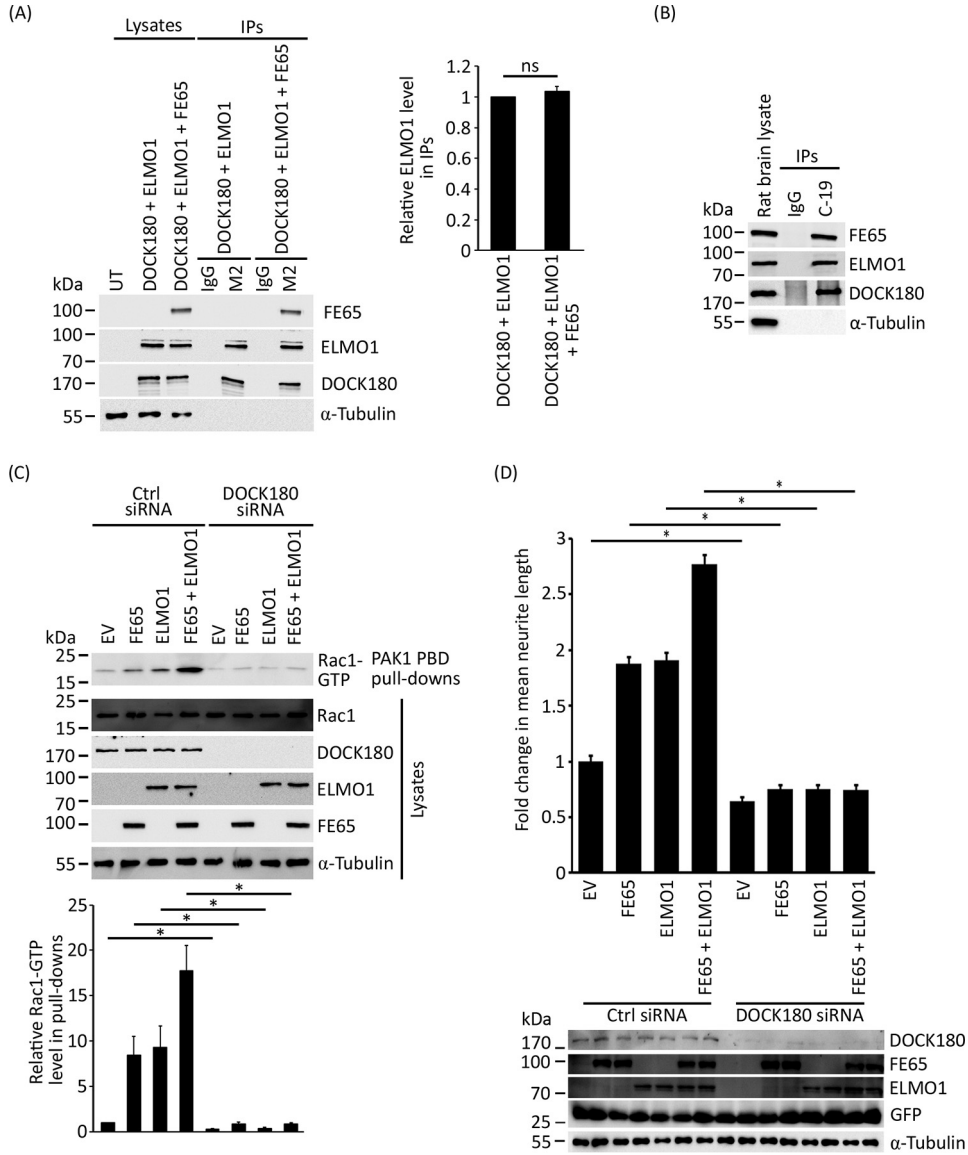


**Figure 4. DOCK180 is required for FE65- and ELMO1-mediated Rac1 activation and neurite outgrowth.** *A*, DOCK180, ELMO1, and FE65 interact in immunoprecipitation assays from transfected cells. Immunoprecipitations were performed from CHO cells transfected with DOCK180 + ELMO1 and DOCK180 + ELMO1 + FE65. DOCK180 was immunoprecipitated using anti-FLAG against the FLAG tag on DOCK180. DOCK180 in the immunoprecipitates was detected by anti-DOCK180 C-19 (1:2500), and ELMO1, FE65, and α-tubulin were detected by anti-ELMO1 PA5-28406, anti-FE65 E20, and anti-α-tubulin DM1A, respectively. *IgG* and *M2* refer to the presence of mouse control IgG and anti-FLAG M2 in the immunoprecipitations, respectively. ELMO1 level in IPs was measured and analyzed as described in the legend to Fig. 1. The relative ELMO1 level in IP was expressed as a densitometric ratio of ELMO1in IP/DOCK180 in IP. Data for graphs were obtained from three independent experiments. *ns*, $p > 0.05$. Results are means ± S.D. (*error bars*). *B*, DOCK180, ELMO1, and FE65 form a complex at the endogenous level. DOCK180 was immunoprecipitated from rat brain lysate using goat anti-DOCK180 C-19. The immunoprecipitates were analyzed for the presence of DOCK180, ELMO1, FE65, and α-tubulin by using anti-DOCK180 C-19 (1:1000), anti-ELMO1 PA5–28406 (1:500), anti-FE65 E20 (1:1000), and anti-α-tubulin DM1A (1:5000), respectively. *IgG* and *C-19* refer to the presence of goat control IgG and anti-DOCK180 C-19 in the immunoprecipitations, respectively. *C*, CHO cells were transfected with the constructs EV control plasmid, FE65, and ELMO1 and either control or DOCK180 siRNAs, as indicated. Rac1 activation assays were performed as described in the legend to Fig. 3. Knockdown of DOCK180 reduces the effects of FE65, ELMO1, and FE65 + ELMO1 on Rac1 activation. In *C*, the relative Rac1-GTP level was expressed as a densitometric ratio of Rac1-GTP/total Rac1. Data for graphs were obtained from three independent experiments. *, $p < 0.001$. Results are means ± S.D. (*error bars*). *D*, rat primary cortical neurons were transfected with the constructs EV control plasmid and different combinations of FE65, ELMO1, control siRNA, and DOCK180 siRNA, as indicated, for the neurite outgrowth assay. Knockdown of DOCK180 suppresses the stimulatory effects of FE65, ELMO1, and FE65 + ELMO1 on neurite outgrowth. The expressions of EGFP, FE65-Myc/Myc-ELMO1, and DOCK180 were determined by Western blot analysis using anti-GFP JL-8 (1:5000), anti-Myc 9B11 (1:2500), and anti-DOCK180 C-19 (1:2500), respectively. α-Tubulin in the lysates was determined by α-tubulin DM1A antibody (1:5000). Data were obtained from at least 40 cells/transfection, and the experiments were repeated three times. *, $p < 0.001$. *Error bars*, S.E.

(Fig. 6*C*). This observation further suggests that FE65 could interfere with ELMO1 autoinhibitory conformation.

It is proposed that ELMO1 activation is a prerequisite for its plasma membrane targeting and Rac1 activation there (7, 8). Thus, we tested whether FE65 alters plasma membrane recruitment of ELMO1. Intriguingly, knockdown of FE65 reduced the amount of both transfected and endogenous ELMO1 in the plasma membrane elutions (Fig. 7, *A* and *B*). Similarly, knockdown of FE65 decreased the number of cells with ELMO1 plasma membrane localization significantly (Fig. 7*F*). Moreover, FE65m decreased the amount of ELMO1 in the plasma membrane elution as compared with the WT counterpart

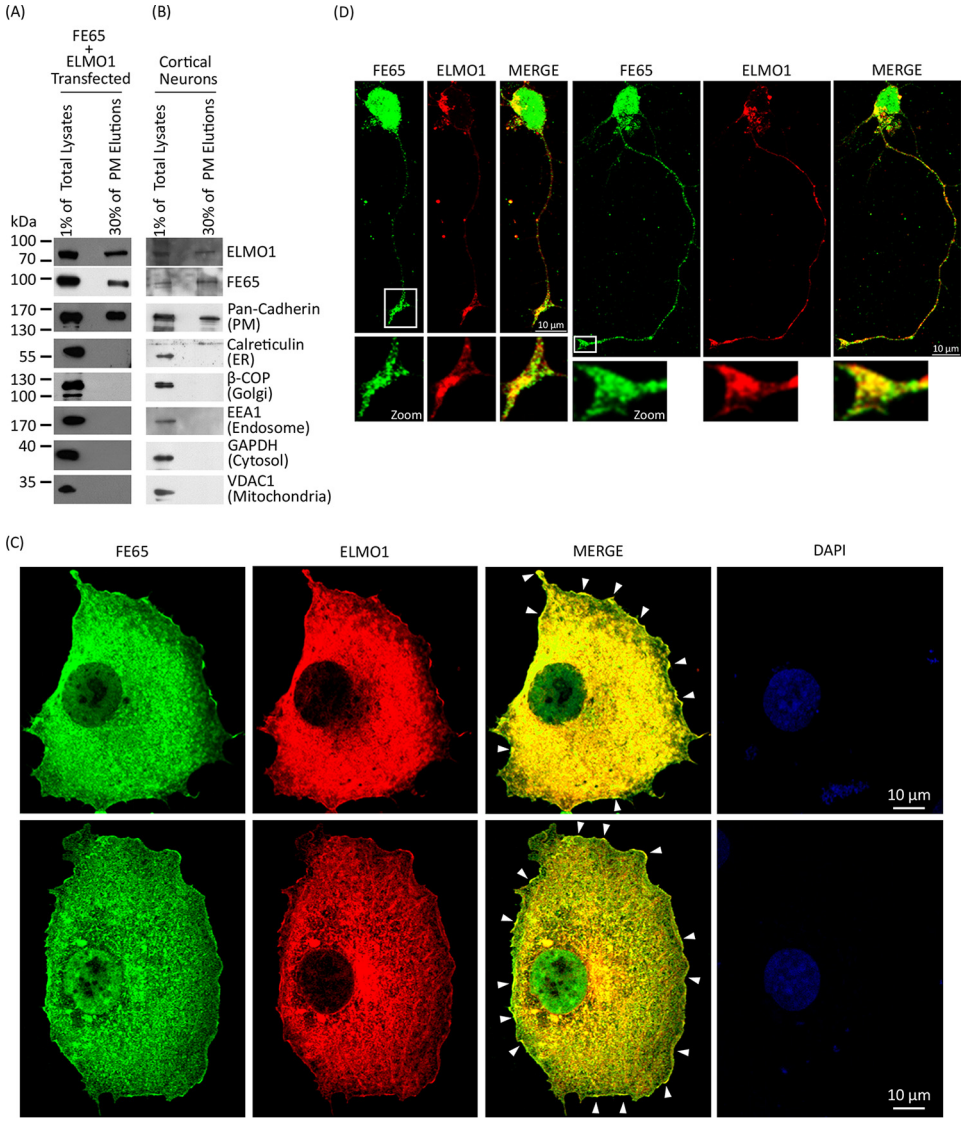


**Figure 5. Co-localization of FE65 and ELMO1 in transfected cells and neurons.** Plasma membrane was isolated from FE65 and ELMO1 co-transfected CHO cells (*A*) and rat primary cortical neurons (*B*) by using a Qproteome plasma membrane protein kit (Qiagen). Approximately 1% of total lysate and 30% of PM elutions were analyzed by immunoblotting by using anti-FE65 E20 (1:1000), anti-ELMO1 B-7 (1:500), and various subcellular compartment marker antibodies, including pan-cadherin (1:2000), calreticulin (1:1000), β-COP (1:1000), EEA1 (1:1000), GAPDH (1:5000), and VADC1 (1:5000). *C*, immunofluorescent staining of COS7 cells transfected with ELMO1 and FE65-Myc. ELMO1 and FE65-Myc were stained by goat anti-ELMO1 N-20 (1:100) and mouse anti-Myc antibody 9B11 (1:1000). An overlaid image is shown. Nuclei were labeled by DAPI. *Scale bar*, 10 μm. Similar to other reports, FE65 is observed in both cytoplasm and nucleus. ELMO1 is mainly located in the cytoplasm. The two proteins are mainly co-localized in the perinuclear region. A proportion of ELMO1 and FE65 are co-localized on the plasma membrane (*pointed*). Both FE65 and ELMO1 are expressed on the plasma membrane. *D*, FE65 and ELMO1 are co-localized in growth cones. Rat cortical neurons were immunostained at day 3 *in vitro* for endogenous FE65 and ELMO1 by a rabbit anti-FE65 (1:100) and a mouse anti-ELMO1 B-7 (1:100). The *enlarged areas* of *boxes* with growth cones are shown. *Scale bar*, 10 μm. In *C* and *D*, two representative cells are shown.

(Fig. 7*C*). These observations may indicate that FE65-ELMO1 interaction is required, at least in part, for targeting of ELMO1 to the plasma membrane. On the other hand, knockdown of ELMO1 did not have a significant effect on the plasma membrane localization of FE65 in both biochemical plasma membrane isolation (Fig. 7, *D* and *E*) and immunofluorescence analyses (Fig. 7*G*). Collectively, our findings suggest that FE65 interacts with ELMO1 to release ELMO1 autoinhibition constraints and facilitates the targeting of ELMO1 to the plasma membrane to stimulate Rac1 signaling.

## Discussion

In the present study, ELMO1 is identified as a novel interactor for the neuronal adaptor protein FE65. A number of interactors are reported for the conserved domains of FE65. To our knowledge, ELMO1 is the first reported FE65 NTR interactor. In addition to FE65, two closely related isoforms, FE65L1 and FE65L2, are identified. Although functional redundancy between FE65 proteins is suggested, there is evidence that FE65 may have some specific biological roles. For instance, only FE65 is capable to mediate FE65-AICD transactivation but not the other two isoforms (reviewed in Ref. 25). Moreover, learning and memory deficits are observed in FE65 single knockout mice, which suggests that FE65L1 and FE65L2 may not be able to fully compensate for some unique FE65 brain functions (3). It is noteworthy that all three FE65 proteins contain a WW and two PTB domains, and their structural divergence occurs pri-

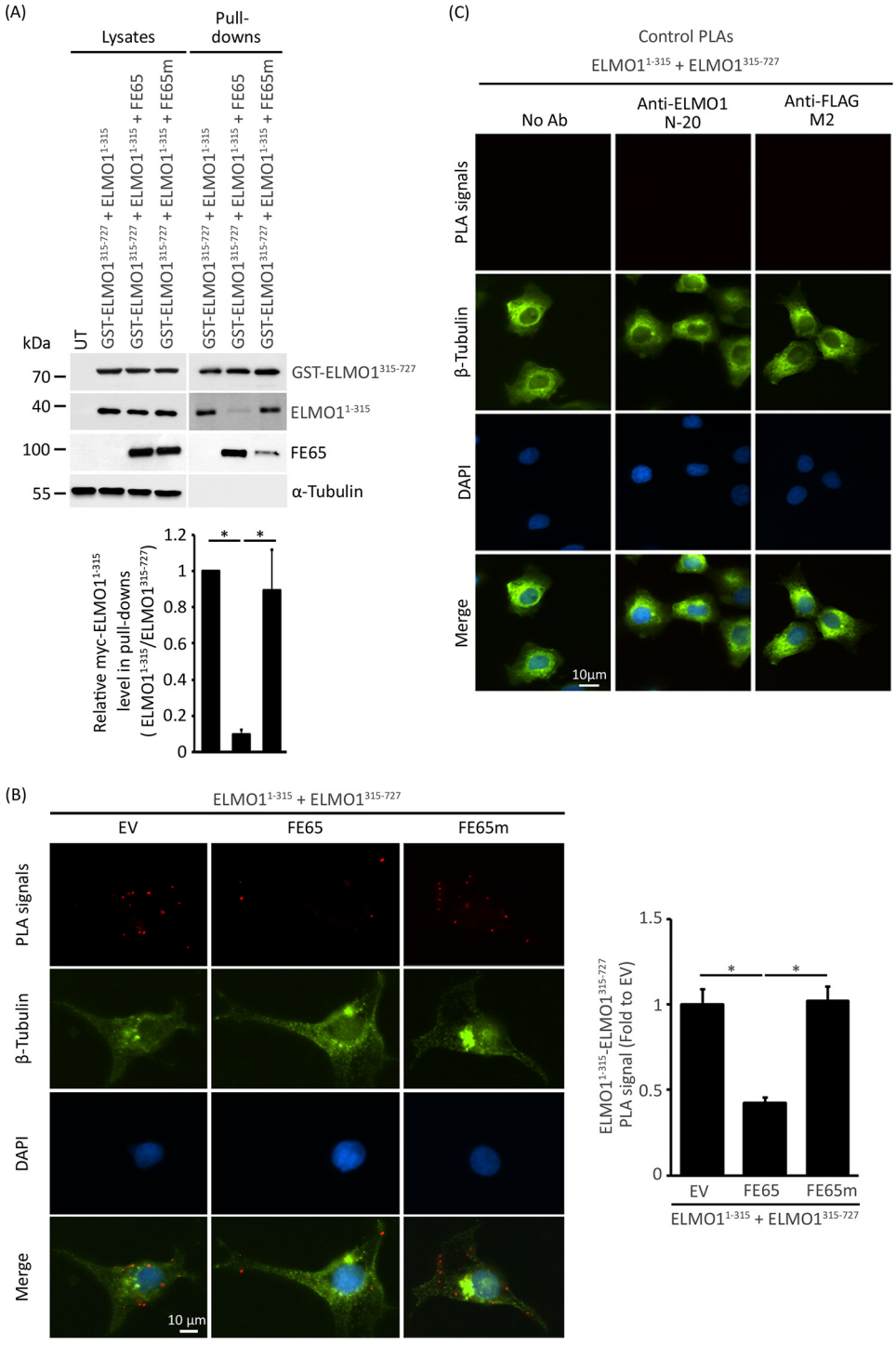


**Figure 6. FE65 releases ELMO1 autoinhibitory conformation.** *A*, FE65, but not FE65m, reduces the intramolecular interaction of ELMO1 EID and EAD in GST pulldown assays. GST-ELMO1(315–727) and Myc-ELMO1(1–315) were transfected into cells with either EV, FE65, or FE65m. GST-ELMO1(315–727) was pulled down from the cell lysates by GSH-Sepharose 4B. The lysates and pull-downs were analyzed for GST-ELMO1(315–727), Myc-ELMO1(1–315), FE65, and α-tubulin by immunoblotting using anti-GST, anti-Myc, anti-FE65, and anti-α-tubulin as stated in the legend to Fig. 1, respectively. Data were obtained from three independent experiments. *, $p < 0.001$. Results are means ± S.D. (*error bars*). *B*, FE65, but not FE65m, reduces the intramolecular interaction of ELMO1 in PLA. Myc-ELMO1(1–315) and FLAG-ELMO1(315–727) were transfected into the cells with EV, FE65, or FE65m. Anti-ELMO1 N-20 (which recognizes Myc-ELMO1(1–315)) or anti-FLAG M2 (which recognizes FLAG-ELMO1(315–727)) were used as primary antibodies for the assays. Reduced ELMO1(1–315)-ELMO1(315–727) PLA signals were observed in the cells co-transfected with FE65 as compared with the cells co-transfected with EV or FE65m. Representative images are shown. *Scale bar*, 10 μm. Cells were stained with β-tubulin (1:200) and DAPI as morphology and nucleus markers, respectively. The *bar chart* shows the relative PLA signal (-fold compared with EV) in different transfections. Data were obtained from at least 60 cells per transfection, and the experiments were repeated three times. *, $p < 0.001$. *Error bars*, S.E. *C*, control PLAs were performed by transfecting Myc-ELMO1(1–315) and FLAG-ELMO1(315–727) to cells. PLAs were performed for either no antibody (*No Ab*), anti-ELMO1 N-20, or anti-FLAG M2. No PLA signal was observed in all of the samples. Cells were also stained with β-tubulin and DAPI as morphology and nuclear markers, respectively. *Scale bar*, 10 μm.

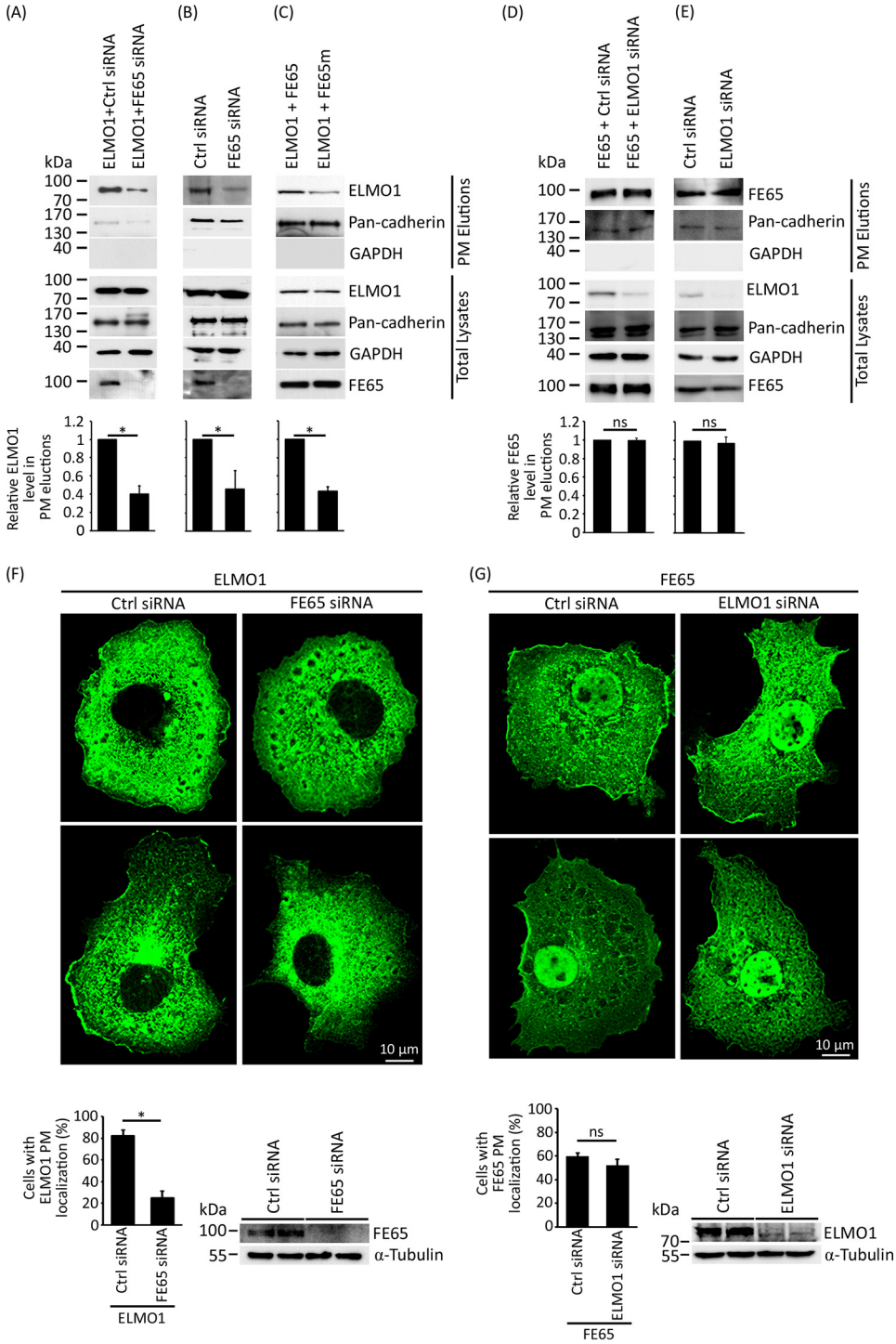


**Figure 7. FE65 is required for the plasma membrane targeting of ELMO1.** PM was isolated from CHO cells transfected with either ELMO1 + control siRNA or ELMO1 + FE65 siRNA (*A*), control siRNA or FE65 siRNA (*B*), ELMO1 + FE65 or ELMO1 + FE65m (*C*), FE65 + control siRNA or FE65 + ELMO1 siRNA (*D*), or control siRNA or ELMO1 siRNA (*E*). Knockdown of FE65 reduced the level of transfected (*A*) and endogenous (*B*) ELMO1 in the PM elutions. Overexpression of FE65m decreases the amount of ELMO1 in the PM elution (*C*). Knockdown of ELMO1 did not show any significant effect on the amounts of transfected (*D*) and endogenous (*E*) FE65 in the PM elutions. In *A–E*, pan-cadherin and GAPDH serve as plasma membrane and cytosol markers, respectively. 30% of plasma membrane elution of each treatment was analyzed as described in the legend to Fig. 5. ELMO1 level in the PM elution and total ELMO1 level in the lysate were measured and analyzed as described in the legend to Fig. 5. The relative ELMO1 level in PM elution was expressed as a densitometric ratio of ELMO1 in PM/total ELMO1 in the lysate. Data for graphs were obtained from three independent experiments. *, $p < 0.001$; *ns*, $p > 0.05$. Results are means ± S.D. (*error bars*). COS7 cells were transfected with ELMO1 + control siRNA or ELMO1 + FE65 siRNA (*F*) or with FE65 + control siRNA or FE65 + ELMO1 siRNA (*G*). Cells in *F* and *G* were then immunostained for ELMO1 and FE65 as described in the legend to Fig. 5. The number of cells with or without ELMO1 (*F*) and FE65 PM (*G*) were counted. Two representative cells are shown. Knockdown of FE65 and ELMO1 were confirmed by Western blot analysis. Three independent experiments were performed, and at least 50 cells were counted in each experiment. Data are expressed as percentage of cells with ELMO1 (*F*) and FE65 PM (*G*) localization. *, $p < 0.001$; *ns*, $p > 0.05$. *Error bars*, S.D. (*error bars*).

marily in their NTR. Thus, FE65 NTR may be required for its unique functions. In fact, emerging evidence reveals that FE65 NTR has distinct cellular roles. For instance, an N-terminal truncated FE65 product, named p65FE65, has been identified, and the truncated form has a stronger interaction with several FE65 interactors than the full-length counterpart. Moreover, the truncated FE65 has a more potent effect on suppression of sAPP$\alpha$ secretion and reduced transactivation capability (26). The identification of ELMO1 as an FE65 NTR interactor provides evidence that the FE65 NTR could also function in recruiting proteins for modulating FE65 functions.

Previously, we have shown that FE65 stimulates Rac1 activation (6). Because it does not possess any GEF activities, the exact mechanism(s) by which FE65 promotes Rac1 signaling remains elusive. Intriguingly, we show here that FE65 interacts directly with ELMO1, a regulatory subunit of the ELMO1-DOCK180 Rac1 GEF complex, and knockdown of either ELMO1 or DOCK180 decreases the stimulatory effect of FE65 on Rac1 activation. These findings suggest that FE65 activates Rac1, at least in part, via ELMO1-DOCK180 Rac1 GEF.

Here, we also show that Met-692 and Glu-693 within ELMO1 EAD are essential for FE65-ELMO1 interaction in both Y2H and co-immunoprecipitation assays. The two residues are also crucial for mediating ELMO1 EID-EAD intramolecular interaction (15). These suggest that both FE65 and ELMO1 EID bind to a similar region on the ELMO1 EAD. It is noteworthy that ELMO1 adopts an inactive closed conformation by its EID-EAD interaction at basal state, and release of such constraints is required for proper functioning of DOCK180 in Rac1 activation (15). Although it has long been proposed that ELMO1 interactors play a part in relieving ELMO1 autoinhibition (reviewed in Refs. 7 and 13), such a molecule was yet to be identified. Our findings reveal that FE65 is an interactor of ELMO1 EAD to diminish ELMO1 EID-EAD intramolecular inhibitory interaction. Of note, overexpression of either FE65 or ELMO1 also stimulates Rac1 activation and neurite outgrowth. This may be due to the exogenous proteins interacting with the endogenous partners, as both FE65 and ELMO1 are expressed in the cells used in this study (Fig. 2*A*). As mentioned above, once the two proteins interact, FE65 releases ELMO1 autoinhibition conformation. The FE65-ELMO1 complex becomes "active" for the downstream activities, such as Rac1 activation. Hence, it is essential to identify the upstream mechanism(s) that regulates FE65-ELMO1 interaction. It is reported that phosphorylation modulates the interactions between FE65 and its interactors (27–29). Therefore, it is possible that phosphorylation of FE65 and/or ELMO1 regulates their interaction and thereby FE65-ELMO1 complex activation.

In addition to ELMO1, FE65 has been shown to bind to ARF6, a small GTPase implicated in various neuronal processes, including axonal elongation (6, 30, 31). The effects of ARF6 are attributed, at least in part, by activation of Rac1. However, the exact mechanism by which ARF6 stimulates Rac1 remains unclear. Of note, ARF family members have been shown to form multimeric complexes to activate various biological events. For example, a multimeric complex that contains clathrin, ARF1, AP1, and CYFIP is reported to play a significant regulatory role in clathrin-AP1– coated carrier biogenesis (32). Additionally, several GTPases and their GTPase-activating proteins complex with ARF4 for the ciliary trafficking of polycystin-1 (33). Although ARF6 activation is reported to stimulate Rac1 signaling through the ELMO1-DOCK180 complex (34), the linkage between ARF6 and the ELMO1-DOCK180 complex was unknown. Therefore, it is worth investigating whether FE65 functions as a link to orchestrate ARF6 and ELMO1-DOCK180 for stimulating Rac1 signaling.

It is noteworthy that deregulation of Rac1, a well-known Rho family small GTPase, has been implicated in a variety of diseases, including, but not limited to, cancer, cardiovascular diseases, and neurodegenerative disorders (35). For instance, defective Rac1 signaling is associated with Alzheimer's disease and motor neuron disease (36–38). These diseases are characterized by synaptic loss and dysfunction. Of note, FE65 has been implicated in synaptic functions (5, 6, 39, 40), and reduced FE65 expression is observed in both Alzheimer's disease and motor neuron disease (41, 42). Signaling pathways that regulate embryonic neurite development are conserved in adults for controlling synaptic plasticity, including Rac1 signaling (43). Because we show here that FE65 regulates Rac1 activity by recruiting ELMO1, dysfunction of FE65 may play a role in the pathogenesis of Alzheimer's disease and motor neuron disease.

Increasing evidence suggests roles of FE65 in cancer. For example, FE65 expression is reported to be increased in thyroid carcinomas, which could stimulate cancer cell growth by promoting sAPP generation (44, 45). Moreover, FE65 has been shown to enhance the transcriptional activity of estrogen receptor $\alpha$ and to stimulate breast cancer cell growth (46). Additionally, it has been reported that FE65 suppresses the migration and invasion of estrogen receptor $\alpha$–negative breast cancer cells (47). In addition to neuronal functions, our finding opens an avenue for studying the association between FE65, Rac1 signaling, and carcinogenesis, which may lead to novel therapeutic targets for intervention. Altogether, we show that FE65 interacts with ELMO1-DOCK180 to stimulate Rac1-mediated neurite outgrowth by activating ELMO1 (Fig. 8).

## Experimental procedures

### *Plasmids*

Mammalian expression constructs for WT FE65 and Myc-tagged FE65 were as described (48–50). FE65 K48A/R51A (FE65m) mutant was generated by using the QuikChange II site-directed mutagenesis kit (Agilent Technologies). The mammalian expression construct of Myc-tagged ELMO1, FLAG-tagged ELMO1, and FLAG-tagged DOCK180 are gifts from Prof. Jean-François Côté (51), Prof. Kodi S. Ravichandran (52), and Prof. Michiyuki Matsuda (53), respectively. Yeast bait constructs of FE65 contain residues 1–217, 1–95, 1–60, and 61–217 were generated by subcloning the corresponding FE65 cDNA into pGBKT7. Myc-tagged ELMO1(1–315) was created by introducing a stop codon after ELMO1 residue 315 in the Myc-tagged ELMO1 construct using the QuikChange II site-directed mutagenesis kit. FLAG-tagged ELMO1(315–727) and GST-tagged ELMO1(315–727) were generated by subcloning the corresponding cDNA into pCMV-Tag2B (Agilent Technol-

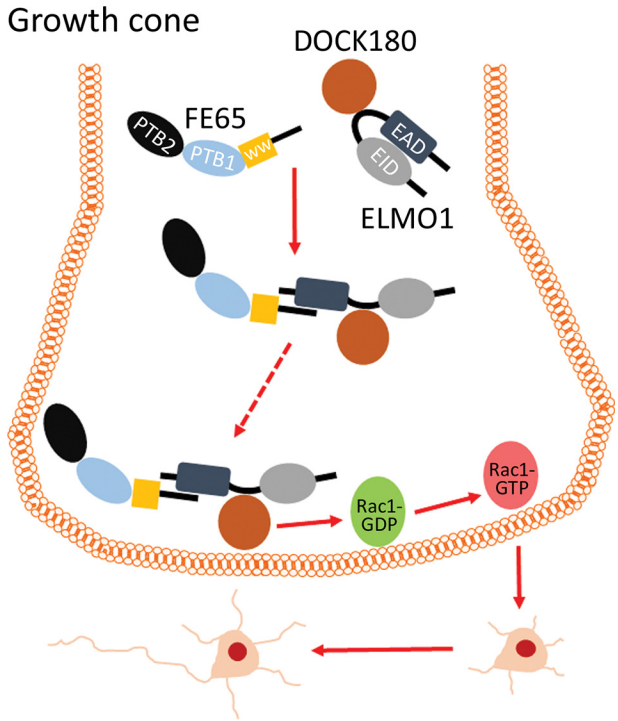


**Figure 8. A schematic diagram illustrates the role of FE65-ELMO1 interaction.** In the growth cone, FE65 recruits ELMO1-DOCK180 bipartite Rac1 GEF complex and activates ELMO1 by disrupting its autoinhibitory closed conformation from between EID and EAD. Once activated, the FE65-ELMO1-DOCK180 complex is targeted to the plasma membrane to promote Rac1 activation and thereby neurite outgrowth.

ogies) and pCIneo-GST (6), respectively. Yeast prey constructs of ELMO1 containing residues 626–727 and 626–680 were generated by subcloning the corresponding ELMO1 cDNA into pGADT7-RecAB. Both mammalian and yeast constructs for ELMO1 M692A/E693A mutant were generated by mutagenesis. The bacterial GST fusion protein construct of ELMO1 (626–727) was prepared by subcloning of the ELMO1 corresponding cDNA into pGEX-6P-1 (GE Healthcare).

### *Antibodies*

Rabbit anti-FE65 was as described (27); goat anti-FE65 (E20) was obtained from Santa Cruz Biotechnology, Inc.; and mouse anti-FE65 (4H324) was from Abcam. Rabbit anti-ELMO1 (PA5–28406) was from Thermo Fisher Scientific. Goat (N-20) and mouse (B-7) anti-ELMO1 were purchased from Santa Cruz Biotechnology. Anti-calreticulin (D3E6), mouse (9B11), and rabbit (71D10) anti-Myc antibodies were purchased from Cell Signaling Technology. Anti-polyhistidine (HIS-1), anti-GST, anti-FLAG (M2), anti-pan-cadherin (C1821), and β-COP (G6160) were purchased from Sigma. Anti-Rac1 (23A8) was obtained from Millipore. Anti-ARF6 (3A-1), anti-DOCK180 (C-19), and anti-α-tubulin antibody (DM1A) were purchased from Santa Cruz Biotechnology. Anti-VDAC1 (ab15895) and anti-β-tubulin antibody (ab6046) were obtained from Abcam. Anti-GFP (JL-8), anti-GAPDH (AM4300), and anti-EEA1 antibody (610456) were purchased from Clontech, Ambion, and BD Transduction Laboratories, respectively. Mouse and goat IgG controls were purchased from Thermo Fisher Scientific.

### *Yeast two-hybrid system*

A yeast two-hybrid screen of the mouse brain Mate and Plate cDNA library (Clontech) was performed essentially as described previously, using the cDNA that encodes for the human FE65 amino acids 1–217 as bait (6). β-gal colony-lift filter assays were performed essentially as described previously (54).

For mapping the interacting regions, various pGBKT7-FE65 bait and pGADT7-ELMO1 prey constructs were co-transformed into yeast Y2H Gold and then grew on double (−Leu/−Trp) and quadruple (−Ade/−His/−Leu/−Trp) dropout SD agar plates.

### *Cell culture and transfection*

CHO, HEK293, and E18 primary rat cortical neurons were prepared and cultured as described previously (6, 54).

For plasmid transfection, CHO and HEK293 cells were transfected with X-tremeGENE™ 9 (Roche Applied Science), and rat cortical neurons were transfected with Lipofectamine 2000 (Thermo Fisher Scientific) according to the manufacturers' instructions and as described previously (6). Accell siRNAs and regular siRNAs were obtained from GE Dharmacon. siRNAs were transfected to CHO and HEK293 by using Lipofectamine RNAiMAX (Thermo Fisher Scientific).

### *Protein-binding assays*

The GST and GST fusion proteins were expressed in *E. coli* BL21 and captured by GSH-Sepharose 4B resin according to the manufacturer's instructions (GE Healthcare). The expressed proteins were used as "baits" in GST pulldown assays as described (6, 27, 54). Co-immunoprecipitation assays were performed essentially as described previously from transfected cell and rat brain lysates (6, 27, 54).

Direct binding assays were performed as described previously (6, 54). In brief, GST and GST-ELMO1(626–727) were expressed and purified from *E. coli*. The GST baits were used to pull down purified His-FE65(1–217). The protein complexes were captured by GSH-Sepharose 4B resin and then analyzed by SDS-PAGE and Western blotting.

### *Rac1 activation assays*

Rac1-GTP levels in cells were determined by using a Rac1 activation assay kit (Thermo Scientific) as described previously (6). The relative amount of Rac1-GTP in PAK-PBD pulldowns was expressed as a densitometric ratio of Rac1-GTP/total Rac1.

### *Densitometric analysis of Western blots*

Densitometric analysis of Western blots was performed by C-DiGit blot scanner (LI-COR) and analyzed by LI-COR® Image Studio™ software. Data were obtained from at least three independent experiments.

### *Immunofluorescence studies and neurite length measurements*

Immunofluorescence staining and neurite length measurement were performed as described previously (6, 54). Three independent experiments, with at least 40 neurons each, were

performed in a blind manner. The lengths were determined as the distance from the growth cone tip to the periphery of the cell body and quantified using ImageJ (National Institutes of Health) with the NeuronJ plugin (55). For the co-localization study, intensity correction analyses were performed as described using ImageJ with the JAcoP plugin (6, 20, 21). Three independent experiments with at least 40 cells were analyzed. Statistical analyses were performed using a one-way analysis of variance test with the Bonferroni post hoc test. Differences were considered significant at $p < 0.05$.

### *Plasma membrane isolation*

Plasma membrane was isolated from cells by using a Qproteome plasma membrane protein kit (Qiagen). Briefly, cells were harvested in ice-cold PBS and then washed with 1× lysis buffer PM two times. Cell pellets were lysed in 1× lysis buffer PM with protease inhibitors and lysis solution PL at 4 °C for 15 min. The lysates were then cleared by centrifugation at 4 °C, 450 × *g* for 5 min. Supernatants were incubated with binding ligand PBL and Strep-Tactin magnetic beads at 4 °C for 1 h. The magnetic beads were washed with lysis buffer PM and followed by wash buffer twice. The isolated plasma membrane proteins were eluted by boiling in 1× SDS sample buffer, and 30% of plasma membrane elutions were subjected to Western blot analysis for FE65 and ELMO1. The purity of the plasma membrane preparations was validated by probing the samples with various subcellular compartment marker antibodies. Approximately 1% of total lysates were loaded for size comparison.

### *Proximity ligation assays*

A PLA was performed by using a Duolink In Situ fluorescence kit (Sigma). In brief, HEK293 cells were seeded on coverslips 24 h before transfection. Mammalian expression constructs Myc-ELMO1(1–315) and FLAG-ELMO1(315–727) were transfected into the cells with EV, FE65, or FE65m. The cells were fixed with 4% paraformaldehyde and permeabilized with 0.1% Triton 24 h post-transfection. After blocking with 5% FBS in PBS at 37 °C for 1 h, the cells were then incubated with goat anti-ELMO1 N-20 (1:100) and mouse anti-FLAG M2 (1:200) for 1 h at room temperature to probe for Myc-ELMO1(1–315) and FLAG-ELMO1(315–727), respectively. The cells were then washed three times with 1× Wash Buffer A, followed by incubation with Duolink In Situ PLA probe anti-mouse PLUS and anti-goat MINUS at 37 °C for 1 h in a humid incubator. After incubation, the cells were washed three times with 1× Wash Buffer A. Ligation was performed by adding 1× ligation stock and diluted ligase at 37 °C for 30 min, followed by two washes with 1× Wash Buffer A. Amplification was carried out in a darkened humid incubator by incubating the cells with 1× amplification stock and diluted polymerase at 37 °C for 100 min. Then the cells were washed two times with 1× Wash Buffer B and then one time with 0.01× Wash Buffer B. The coverslips were mounted with Duolink In Situ mounting medium with 4′,6-diamidino-2-phenylindole (DAPI). Images were captured by using an Olympus IX71 fluorescence microscope with an UPlanSAPo ×60 water immersion objective. Fluorescence images were captured by a Nikon DS-Qi2 camera, and the fluorescence signals were quantified by the Object Count tool in Nikon NIS Elements. Cells were also stained with anti-β-tubulin as a morphology marker.

### *Statistical analyses*

All experiments were repeated at least three times. Statistical analyses were performed using one-way analysis of variance tests with the Bonferroni post hoc test. Significance between different treatments is indicated as follows: *, $p < 0.001$; **, $p < 0.01$; ***, $p < 0.05$; *ns*, not significant ($p > 0.05$). *Error bars* show either S.D. or S.E.

*Author contributions*—W.L., K.M.V.T., W.W.R.C., and A.C.K. performed research. W.L., J.C.K.N., H.Y.E.C., and K.F.L. conceived the study, designed the experiments, analyzed the data, and wrote the paper.

*Acknowledgments—We thank Prof. Jean-François Côté (Montreal Clinical Research Institute), Prof. Kodi S. Ravichandran (University of Virginia School of Medicine), and Prof. Michiyuki Matsuda (Faculty of Medicine, Kyoto University) for the mammalian expression construct of Myc-tagged ELMO1, FLAG-tagged ELMO1, and FLAG-tagged DOCK180, respectively.*

### References

1. Minopoli, G., Gargiulo, A., Parisi, S., and Russo, T. (2012) Fe65 matters: new light on an old molecule. *IUBMB Life* **64,** 936–942 CrossRef Medline
2. Chow, W. N., Cheung, H. N., Li, W., and Lau, K. F. (2015) FE65: roles beyond amyloid precursor protein processing. *Cell Mol. Biol. Lett.* **20,** 66–87 Medline
3. Wang, B., Hu, Q., Hearn, M. G., Shimizu, K., Ware, C. B., Liggitt, D. H., Jin, L. W., Cool, B. H., Storm, D. R., and Martin, G. M. (2004) Isoform-specific knockout of FE65 leads to impaired learning and memory. *J. Neurosci. Res.* **75,** 12–24 CrossRef Medline
4. Guénette, S., Chang, Y., Hiesberger, T., Richardson, J. A., Eckman, C. B., Eckman, E. A., Hammer, R. E., and Herz, J. (2006) Essential roles for the FE65 amyloid precursor protein-interacting proteins in brain development. *EMBO J.* **25,** 420–431 CrossRef Medline
5. Strecker, P., Ludewig, S., Rust, M., Mundinger, T. A., Görlich, A., Krächan, E. G., Mehrfeld, C., Herz, J., Korte, M., Guénette, S. Y., and Kins, S. (2016) FE65 and FE65L1 share common synaptic functions and genetically interact with the APP family in neuromuscular junction formation. *Sci. Rep.* **6,** 25652 CrossRef Medline
6. Cheung, H. N., Dunbar, C., Mórotz, G. M., Cheng, W. H., Chan, H. Y., Miller, C. C., and Lau, K. F. (2014) FE65 interacts with ADP-ribosylation factor 6 to promote neurite outgrowth. *FASEB J.* **28,** 337–349 CrossRef Medline
7. Patel, M., Pelletier, A., and Côté, J. F. (2011) Opening up on ELMO regulation: new insights into the control of Rac signaling by the DOCK180/ELMO complex. *Small GTPases* **2,** 268–275 CrossRef Medline
8. Ravichandran, K. S., and Lorenz, U. (2007) Engulfment of apoptotic cells: signals for a good meal. *Nat. Rev. Immunol.* **7,** 964–974 CrossRef Medline
9. Li, H., Yang, L., Fu, H., Yan, J., Wang, Y., Guo, H., Hao, X., Xu, X., Jin, T., and Zhang, N. (2013) Association between $G\alpha_{i2}$ and ELMO1/Dock180 connects chemokine signalling with Rac activation and metastasis. *Nat. Commun.* **4,** 1706 CrossRef Medline
10. Kim, J. Y., Oh, M. H., Bernard, L. P., Macara, I. G., and Zhang, H. (2011) The RhoG/ELMO1/Dock180 signaling module is required for spine morphogenesis in hippocampal neurons. *J. Biol. Chem.* **286,** 37615–37624 CrossRef Medline
11. Stevenson, C., de la Rosa, G., Anderson, C. S., Murphy, P. S., Capece, T., Kim, M., and Elliott, M. R. (2014) Essential role of Elmo1 in Dock2-dependent lymphocyte migration. *J. Immunol.* **192,** 6062–6070 CrossRef Medline

12. Ridley, A. J. (2006) Rho GTPases and actin dynamics in membrane protrusions and vesicle trafficking. *Trends Cell Biol.* **16,** 522–529 CrossRef Medline
13. Laurin, M., and Côté, J. F. (2014) Insights into the biological functions of Dock family guanine nucleotide exchange factors. *Genes Dev.* **28,** 533–547 CrossRef Medline
14. Komander, D., Patel, M., Laurin, M., Fradet, N., Pelletier, A., Barford, D., and Côté, J. F. (2008) An α-helical extension of the ELMO1 pleckstrin homology domain mediates direct interaction to DOCK180 and is critical in Rac signaling. *Mol. Biol. Cell* **19,** 4837–4851 CrossRef Medline
15. Patel, M., Margaron, Y., Fradet, N., Yang, Q., Wilkes, B., Bouvier, M., Hofmann, K., and Côté, J. F. (2010) An evolutionarily conserved autoinhibitory molecular switch in ELMO proteins regulates Rac signaling. *Curr. Biol.* **20,** 2021–2027 CrossRef Medline
16. Bryan, B., Kumar, V., Stafford, L. J., Cai, Y., Wu, G., and Liu, M. (2004) GEFT, a Rho family guanine nucleotide exchange factor, regulates neurite outgrowth and dendritic spine formation. *J. Biol. Chem.* **279,** 45824–45832 CrossRef Medline
17. Tudor, E. L., Perkinton, M. S., Schmidt, A., Ackerley, S., Brownlees, J., Jacobsen, N. J., Byers, H. L., Ward, M., Hall, A., Leigh, P. N., Shaw, C. E., McLoughlin, D. M., and Miller, C. C. (2005) ALS2/Alsin regulates Rac-PAK signaling and neurite outgrowth. *J. Biol. Chem.* **280,** 34735–34740 CrossRef Medline
18. Lundquist, E. A. (2003) Rac proteins and the control of axon development. *Curr. Opin. Neurobiol.* **13,** 384–390 CrossRef Medline
19. Bustelo, X. R., Ojeda, V., Barreira, M., Sauzeau, V., and Castro-Castro, A. (2012) Rac-ing to the plasma membrane: the long and complex work commute of Rac1 during cell signaling. *Small GTPases* **3,** 60–66 CrossRef Medline
20. Li, Q., Lau, A., Morris, T. J., Guo, L., Fordyce, C. B., and Stanley, E. F. (2004) A syntaxin 1, $G\alpha_o$, and N-type calcium channel complex at a presynaptic nerve terminal: analysis by quantitative immunocolocalization. *J. Neurosci.* **24,** 4070–4081 CrossRef Medline
21. Stoops, E. H., Hull, M., and Caplan, M. J. (2016) Newly synthesized and recycling pools of the apical protein gp135 do not occupy the same compartments. *Traffic* **17,** 1272–1285 CrossRef Medline
22. Nikolic, M. (2002) The role of Rho GTPases and associated kinases in regulating neurite outgrowth. *Int. J. Biochem. Cell Biol.* **34,** 731–745 CrossRef Medline
23. Etienne-Manneville, S., and Hall, A. (2002) Rho GTPases in cell biology. *Nature* **420,** 629–635 CrossRef Medline
24. Sabo, S. L., Ikin, A. F., Buxbaum, J. D., and Greengard, P. (2003) The amyloid precursor protein and its regulatory protein, FE65, in growth cones and synapses *in vitro* and *in vivo*. *J. Neurosci.* **23,** 5407–5415 Medline
25. McLoughlin, D. M., and Miller, C. C. (2008) The FE65 proteins and Alzheimer's disease. *J. Neurosci. Res.* **86,** 744–754 CrossRef Medline
26. Hu, Q., Wang, L., Yang, Z., Cool, B. H., Zitnik, G., and Martin, G. M. (2005) Endoproteolytic cleavage of FE65 converts the adaptor protein to a potent suppressor of the sAPPα pathway in primates. *J. Biol. Chem.* **280,** 12548–12558 CrossRef Medline
27. Lau, K. F., Chan, W. M., Perkinton, M. S., Tudor, E. L., Chang, R. C., Chan, H. Y., McLoughlin, D. M., and Miller, C. C. (2008) Dexras1 interacts with FE65 to regulate FE65-amyloid precursor protein-dependent transcription. *J. Biol. Chem.* **283,** 34728–34737 CrossRef Medline
28. Chow, W. N., Ngo, J. C., Li, W., Chen, Y. W., Tam, K. M., Chan, H. Y., Miller, C. C., and Lau, K. F. (2015) Phosphorylation of FE65 serine-610 by serum- and glucocorticoid-induced kinase 1 modulates Alzheimer's disease amyloid precursor protein processing. *Biochem. J.* **470,** 303–317 CrossRef Medline
29. Lee, Y. S., Chow, W. N. V., and Lau, K. F. (2017) Phosphorylation of FE65 at threonine 579 by GSK3β stimulates amyloid precursor protein processing. *Sci. Rep.* **7,** 12456 CrossRef Medline
30. Jaworski, J. (2007) ARF6 in the nervous system. *Eur J. Cell Biol.* **86,** 513–524 CrossRef Medline
31. Hernández-Deviez, D. J., Roth, M. G., Casanova, J. E., and Wilson, J. M. (2004) ARNO and ARF6 regulate axonal elongation and branching through downstream activation of phosphatidylinositol 4-phosphate 5-kinase α. *Mol. Biol. Cell* **15,** 111–120 Medline
32. Anitei, M., Stange, C., Parshina, I., Baust, T., Schenck, A., Raposo, G., Kirchhausen, T., and Hoflack, B. (2010) Protein complexes containing CYFIP/Sra/PIR121 coordinate Arf1 and Rac1 signalling during clathrin-AP-1-coated carrier biogenesis at the TGN. *Nat. Cell Biol.* **12,** 330–340 CrossRef Medline
33. Ward, H. H., Brown-Glaberman, U., Wang, J., Morita, Y., Alper, S. L., Bedrick, E. J., Gattone, V. H., 2nd, Deretic, D., and Wandinger-Ness, A. (2011) A conserved signal and GTPase complex are required for the ciliary transport of polycystin-1. *Mol. Biol. Cell* **22,** 3289–3305 CrossRef Medline
34. Santy, L. C., Ravichandran, K. S., and Casanova, J. E. (2005) The DOCK180/Elmo complex couples ARNO-mediated Arf6 activation to the downstream activation of Rac1. *Curr. Biol.* **15,** 1749–1754 CrossRef Medline
35. Marei, H., and Malliri, A. (2017) Rac1 in human diseases: the therapeutic potential of targeting Rac1 signaling regulatory mechanisms. *Small GTPases* **8,** 139–163 CrossRef Medline
36. Nadif Kasri, N., and Van Aelst, L. (2008) Rho-linked genes and neurological disorders. *Pflugers Arch.* **455,** 787–797 CrossRef Medline
37. Zhao, L., Ma, Q. L., Calon, F., Harris-White, M. E., Yang, F., Lim, G. P., Morihara, T., Ubeda, O. J., Ambegaokar, S., Hansen, J. E., Weisbart, R. H., Teter, B., Frautschy, S. A., and Cole, G. M. (2006) Role of p21-activated kinase pathway defects in the cognitive deficits of Alzheimer disease. *Nat. Neurosci.* **9,** 234–242 CrossRef Medline
38. Stankiewicz, T. R., and Linseman, D. A. (2014) Rho family GTPases: key players in neuronal development, neuronal survival, and neurodegeneration. *Front. Cell Neurosci.* **8,** 314 Medline
39. Masin, M., Kerschensteiner, D., Dümke, K., Rubio, M. E., and Soto, F. (2006) Fe65 interacts with P2X2 subunits at excitatory synapses and modulates receptor function. *J. Biol. Chem.* **281,** 4100–4108 CrossRef Medline
40. Nensa, F. M., Neumann, M. H., Schrötter, A., Przyborski, A., Mastalski, T., Susdalzew, S., Loosse, C., Helling, S., El Magraoui, F., Erdmann, R., Meyer, H. E., Uszkoreit, J., Eisenacher, M., Suh, J., Guénette, S. Y., *et al.* (2014) Amyloid β a4 precursor protein-binding family B member 1 (FE65) interactomics revealed synaptic vesicle glycoprotein 2A (SV2A) and sarcoplasmic/endoplasmic reticulum calcium ATPase 2 (SERCA2) as new binding proteins in the human brain. *Mol. Cell. Proteomics* **13,** 475–488 CrossRef Medline
41. Kajiwara, Y., Akram, A., Katsel, P., Haroutunian, V., Schmeidler, J., Beecham, G., Haines, J. L., Pericak-Vance, M. A., and Buxbaum, J. D. (2009) FE65 binds Teashirt, inhibiting expression of the primate-specific caspase-4. *PLoS One* **4,** e5071 CrossRef Medline
42. Gómez-Pinedo, U., Villar-Quiles, R. N., Galán, L., Matías-Guiu, J. A., Benito-Martin, M. S., Guerrero-Sola, A., Moreno-Ramos, T., and Matías-Guiu, J. (2016) Immununochemical markers of the amyloid cascade in the hippocampus in motor neuron diseases. *Front. Neurol.* **7,** 195 Medline
43. Martinez, L. A., and Tejada-Simon, M. V. (2011) Pharmacological inactivation of the small GTPase Rac1 impairs long-term plasticity in the mouse hippocampus. *Neuropharmacology* **61,** 305–312 CrossRef Medline
44. Pietrzik, C. U., Hoffmann, J., Stöber, K., Chen, C. Y., Bauer, C., Otero, D. A., Roch, J. M., and Herzog, V. (1998) From differentiation to proliferation: the secretory amyloid precursor protein as a local mediator of growth in thyroid epithelial cells. *Proc. Natl. Acad. Sci. U.S.A.* **95,** 1770–1775 CrossRef Medline
45. Krause, K., Karger, S., Sheu, S. Y., Aigner, T., Kursawe, R., Gimm, O., Schmid, K. W., Dralle, H., and Fuhrer, D. (2008) Evidence for a role of the amyloid precursor protein in thyroid carcinogenesis. *J. Endocrinol.* **198,** 291–299 CrossRef Medline
46. Sun, Y., Kasiappan, R., Tang, J., Webb, P. L., Quarni, W., Zhang, X., and Bai, W. (2014) A novel function of the Fe65 neuronal adaptor in estrogen receptor action in breast cancer cells. *J. Biol. Chem.* **289,** 12217–12231 CrossRef Medline
47. Sun, Y., Sun, J., Lungchukiet, P., Quarni, W., Yang, S., Zhang, X., and Bai, W. (2015) Fe65 suppresses breast cancer cell migration and invasion through Tip60 mediated cortactin acetylation. *Sci. Rep.* **5,** 11529 CrossRef Medline

48. Lau, K. F., McLoughlin, D. M., Standen, C. L., Irving, N. G., and Miller, C. C. (2000) Fe65 and X11$\beta$ co-localize with and compete for binding to the amyloid precursor protein. *Neuroreport* **11,** 3607–3610 CrossRef Medline
49. Perkinton, M. S., Standen, C. L., Lau, K. F., Kesavapany, S., Byers, H. L., Ward, M., McLoughlin, D. M., and Miller, C. C. (2004) The c-Abl tyrosine kinase phosphorylates the Fe65 adaptor protein to stimulate Fe65/amyloid precursor protein nuclear signaling. *J. Biol. Chem.* **279,** 22084–22091 CrossRef Medline
50. Cao, X., and Südhof, T. C. (2001) A transcriptionally [correction of transcriptively] active complex of APP with Fe65 and histone acetyltransferase Tip60. *Science* **293,** 115–120 CrossRef Medline
51. Margaron, Y., Fradet, N., and Côté, J. F. (2013) ELMO recruits actin cross-linking family 7 (ACF7) at the cell membrane for microtubule capture and stabilization of cellular protrusions. *J. Biol. Chem.* **288,** 1184–1199 CrossRef Medline
52. Mauldin, J. P., Lu, M., Das, S., Park, D., Ernst, P. B., and Ravichandran, K. S. (2013) A link between the cytoplasmic engulfment protein Elmo1 and the Mediator complex subunit Med31. *Curr. Biol.* **23,** 162–167 CrossRef Medline
53. Nishihara, H., Kobayashi, S., Hashimoto, Y., Ohba, F., Mochizuki, N., Kurata, T., Nagashima, K., and Matsuda, M. (1999) Non-adherent cell-specific expression of DOCK2, a member of the human CDM-family proteins. *Biochim. Biophys. Acta* **1452,** 179–187 CrossRef Medline
54. Hao, Y., Perkinton, M. S., Chan, W. W., Chan, H. Y., Miller, C. C., and Lau, K. F. (2011) GULP1 is a novel APP-interacting protein that alters APP processing. *Biochem. J.* **436,** 631–639 CrossRef Medline
55. Meijering, E., Jacob, M., Sarria, J. C., Steiner, P., Hirling, H., and Unser, M. (2004) Design and validation of a tool for neurite tracing and analysis in fluorescence microscopy images. *Cytometry A* **58,** 167–176 Medline